Spectra taken in the terrestrial atmosphere and in laboratory mixtures of varying proportions of CO_2 and Ar show a strong peak at 2.96 kev that is caused by Ar K_α x-rays (Fig. 1a). Calibration of the instrument for Ar determinations (Fig. 2) was made by introducing mixtures of CO_2 and Ar in various proportions and at different pressures into a vacuum chamber in which a flight-type x-ray fluorescence spectrometer was installed. Spectra were obtained at three combinations of total pressure and seven different ratios of Ar to CO_2. Appropriate integration limits for the Ar K_α and ^{55}Fe backscatter peak were chosen by inspection. In addition, the instrument on Viking 1 lander was calibrated in an atmosphere (6.9 ± 0.13 mbar) of pure Ar prior to being installed on the spacecraft. After correction for source decay (2.60-year half-life of ^{55}Fe), the instrument sensitivity was 471 count/mbar (69.1 seconds, channels 35 to 50) at the time of landing. The spectral characteristics for 5 percent and 20 percent Ar in CO_2 (8 mbar total pressure) are shown in Fig. 1a. Two days prior to landing a baseline spectrum was taken of the instrument on Viking 1 lander to verify instrument settings. This spectrum, which because of mission constraints was taken at a lower gain than the bulk of the landed spectra, was mathematically expanded and normalized to the backscatter peak. It is presented as a solid line in Fig. 1b for comparison with a smooth curve of the pooled data from three separate scans after landing. No Ar peak is apparent in the spectrum taken after the instrument was landed on Mars. Also not detected are gases containing chlorine (channel 36) or sulfur (channel 30). Over the total measurement period of 6 hours, the temperature at the sample cavity slowly dropped from 25° to 19°C (calibration was at 28°C). Integrated over the Ar peak, the total count measured in situ was virtually identical to that prior to landing. When the above Ar sensitivity is combined with the background count, the Ar concentration determined at the landing site of the Viking 1 lander is less than 0.15 mbar at the 95 percent confidence level. The reported 7.7 mbar total pressure (*8*) at the landing site would place the Ar concentration at not more than 2 percent by volume. This result is in good agreement with the data reported by the entry mass spectrometer (*5*) and the mass spectrometer on the lander (*7*), which reported 1.5 percent and 1 to 2 percent by volume, respectively.

The abundance of Ar in the martian atmosphere reflects (i) the original abundance and (ii) the balance of processes supplying and removing the element from the atmosphere. Because of the high $^{40}Ar/^{36}Ar$ ratio (*5, 7*), most of the atmospheric Ar is radiogenic in origin, having been formed by decay of ^{40}K. Clearly, considerable importance will be attached to the K contents of the martian surface materials analyzed by the x-ray fluorescence spectrometer on the lander, and it is hoped that clues can be provided by the x-ray fluorescence data not only regarding the internal and surficial differentiation of Mars but also regarding the evolution of its atmosphere.

BENTON C. CLARK
Planetary Sciences Laboratory, Martin Marietta Aerospace, Denver, Colorado 80201
PRIESTLEY TOULMIN III
U.S. Geological Survey, Reston, Virginia 22092
A. K. BAIRD
Department of Geology, Pomona College, Claremont, California 91711
KLAUS KEIL
Department of Geology and *Institute of Meteoritics, University of New Mexico, Albuquerque 87123*
HARRY J. ROSE, JR.
U.S. Geological Survey Reston, Virginia 22092

References and Notes

1. P. Toulmin, III, A. K. Baird, B. C. Clark, K. Keil, H. J. Rose, Jr., *Icarus* **20**, 153 (1973).
2. J. S. Levine and G. R. Riegler, *Geophys. Res. Lett.* **1**, 285 (1974); L. D. Kaplan, P. Connes, J. Connes, M. H. Smith, *Trans. Am. Geophys. Union* **56**, 405 (1975); J. S. Levine, *ibid.*, p. 405; *Icarus* **28**, 165 (1976); T. Owen, *ibid.*, p. 171; F. P. Fanale, *ibid.*, p. 179.
3. V. I. Moroz, *Izvestiya*, 28 March 1974; *Icarus* **28**, 159 (1976); V. G. Istomin, K. V. Grechnev, L. N. Ozerov, M. Ye. Slutskiy, V. A. Paulenko, V. N. Tsvetkov, *Kosm. Issled.* **13**, 16 (1975); V. A. Krasnopolsky, *Icarus* **24**, 28 (1975); V. S. Avduevsky, E. L. Akim, V. I. Aleshin, N. F. Borodin, V. V. Kerzhanovich, Ya. V. Malkov, M. Ya. Marov, S. F. Morozov, V. G. Perminov, M. K. Rozhdestvensky, O. L. Riabov, M. I. Subbotin, U. M. Suslov, Z. P. Cheremuchina, V. I. Shkirina, *Kosm. Issled.* **13**, 21 (1975); V. G. Istomin and K. V. Grechnev, *Icarus* **28**, 155 (1976).
4. A. O. Nier, W. B. Hanson, M. B. McElroy, A. Seiff, N. W. Spencer, *Icarus* **16**, 74 (1972).
5. A. O. Nier, W. B. Hanson, A. Seiff, M. B. Mc Elroy, N. W. Spencer, R. J. Duckett, T. C. D. Knight, W. S. Cook *Science* **193**, 786 (1976).
6. D. M. Anderson, K. Biemann, L. E. Orgel, J. Oro, T. Owen, G. P. Shulman, P. Toulmin, III, H. C. Urey, *Icarus* **16**, 111 (1972).
7. T. Owen and K. Biemann, *Science* **193**, 801 (1976).
8. S. L. Hess, R. M. Henry, C. B. Leovy, J. A. Ryan, J. E. Tillman, T. E. Chamberlain, H. L. Cole, R. G. Dutton, G. C. Greene, W. E. Simon, J. L. Mitchell, *ibid.*, p. 788.
9. Essential contributions to the design, construction, and operation of the Viking x-ray fluorescence spectrometer were made by A. Castro and W. Kelliher. R. R. Moore ran laboratory argon calibrations. C. D. Rowe and R. P. Christian performed data reduction. J. L. Gooding and P. H. Evans assisted in analyzing the calibration data. This work was supported in part by NASA (Viking Program), grants NAS 1-11855, NAS 1-11858, L-9717, and NAS 1-9000. We thank S. Dwornik for his continuing help and assistance.

29 July 1976

Physical Properties of the Martian Surface from the Viking 1 Lander: Preliminary Results

Abstract. *The purpose of the physical properties experiment is to determine the characteristics of the martian "soil" based on the use of the Viking lander imaging system, the surface sampler, and engineering sensors. Viking 1 lander made physical contact with the surface of Mars at 11:53:07.1 hours on 20 July 1976 G. M. T. Twenty-five seconds later a high-resolution image sequence of the area around a footpad was started which contained the first information about surface conditions on Mars. The next image is a survey of the martian landscape in front of the lander, including a view of the top support of two of the landing legs. Each leg has a stroke gauge which extends from the top of the leg support an amount equal to the crushing experienced by the shock absorbers during touchdown. Subsequent images provided views of all three stroke gauges which, together with the knowledge of the impact velocity, allow determination of "soil" properties. In the images there is evidence of surface erosion from the engines. Several laboratory tests were carried out prior to the mission with a descent engine to determine what surface alterations might occur during a Mars landing. On sol 2 the shroud, which protected the surface sampler collector head from biological contamination, was ejected onto the surface. Later a cylindrical pin which dropped from the boom housing of the surface sampler during the modified unlatching sequence produced a crater (the second Mars penetrometer experiment). These two experiments provided further insight into the physical properties of the martian surface.*

General description of the landing area. The specific physical properties of the martian surface at the landing site relevant to the physical properties of the martian surface must be considered in the broader context based on the use of Viking orbiter images and the general scene viewed by the lander cameras in order to achieve balanced interpretations (*1*). Orbital images of the entire Chryse area viewed by Viking 1 orbiter clearly revealed that the uppermost martian surface has been modified by wind. In the immediate vicinity of the initial site (19.5°N, 34°W), images revealed what appeared to be volcanic cones, necks, dikes, dark flows, and both ridges and depressions controlled by conjugate joint sets in a dark layer of probable volcanic origin—the stark relief of these features attested to erosional processes. In the northern part of Chryse (20°N, 35°W) small dark halo craters (approximately 600 m in diameter) surrounded by a lighter background indicated that dark material was excavated by impact cratering and deposited on a lighter surface material which presumably had been deposited or modified by the wind. Some craters had bright wind tails on their southwestern sides, confirming aeolian modification of the surface materials.

Likewise, farther to the northwest at the actual landing site, the surface displayed evidence of deflation and erosion as well as deposition by the wind. Here too, small craters, hundreds of meters in diameter, had excavated material from a dark layer, and were subsequently modified by the wind, producing bright wind tails on the southwestern sides of the craters and stripping the northwestern flanks.

Of equal importance to the physical properties of the surface are the ubiquitous impact craters ranging in size from 200 m to several tens of kilometers in diameter. These craters evidently ejected to great distances large blocks, fragments, crushed rock, and frothy chunks of shocked rocks. Thus, the general setting for the description of physical properties of the martian landing site is a surface material of crater ejecta modified by aeolian processes.

Lander camera images confirm the interpretation of the Viking orbiter images (*2*). The Viking lander camera images reveal a panorama similar to that seen in the southwestern parts of the United States; the large number of blocks and fragments were reminiscent of some lunar surfaces such as areas on the flank of the crater Tycho where Surveyor 7 landed (*3*). Thus, an initial impression of the martian surface is that it is intermediate between a lunar mare and a terrestrial aeolian environment. As in the orbiter images, there is evidence for a northeasterly wind which has produced deflation hollows on the northeastern sides of the rocks and left aerodynamically shaped ridges pointing downward toward the southwest. The detailed character of the physical properties of the martian surface materials are discussed below.

Fig. 1. Lander camera image of the surface near footpad 3, showing the general character of surface and the crater produced by the impact of the shroud (event L.L.T. 002 102950; Fr 12 A 013/002; sun elevation angle is 65.5°, sun is to the right). The width of the footpad shown is 20 cm.

Surface erosion by descent engines. In the site alteration studies simulated in 1971 (*4*), an 18-nozzle descent engine similar to those on the Viking lander was fired while it was lowered at a rate of about 1.52 m/sec (5 feet/sec) from a height of about 12.2 m (40 feet) above a soil bed. The thrust employed was 667 newtons (150 pounds), and the chamber pressure was that of the Mars surface in a carbon dioxide atmosphere.

Viking 1 descended on Mars at about 2.44 m/sec at a thrust of about 743 newtons per engine so that, although the descent velocity and thrust employed in the 1971 site alteration studies are both slightly low, they are not dissimilar to those involved in the Viking 1 landing. At the present, the best estimate of the mechanical properties of the Viking 1 landing site is that they are consistent with a material somewhat stronger or denser, or both, than the "lunar nominal" soil (*5*) used, among others, for preflight site alteration tests.

During the tests, observations were made of the depth and extent of the crater formed in the soil below the descent engine, and the amount and distribution of the soil removed from the crater. In addition, before each test firing, rocks of varying sizes and other features such as model craters, troughs, and ridges were placed or located at different distances from the engine descent axis.

In the lunar nominal soil the area below the descent engine was scrubbed and some soil removed to a depth of a few millimeters, but no distinct crater was formed. Finer grains were removed until coarse particles were exposed at the soil surface, giving the appearance of a fine-grained lag gravel. No sign of separate craters caused by the individual engine nozzles was apparent. By contrast, in the dune sand (*6*) individual craters were visible in a general broad erosion crater up to a centimeter deep. Furthermore, regions of the lunar nominal soil which had been prepared (*7*) at lower density than the bulk of the test bed showed no difference in erosion. This finding indicates that the soil's grain size is more important in the erosion process than its density.

During the surface alteration tests, blowing dust was observed as soon as the descent engine was ignited at 12.2 m above the soil surface. The test area was totally obscured by blowing dust after engine shutdown and several minutes were required for the chamber to clear. It seems likely, on the basis of the presence of fine-sized grains on Mars, that the dust cloud caused by the landing would also last several minutes in view of the lower Mars gravity. Subsequent meteorological observations (*8*) indicate that, for the most part, the prevailing winds at the landing site of the Viking 1 lander blow from the northeast at a few meters per second. At the time of landing, the sun was in the southwest. Thus the dust cloud generated by the landing would drift to the southwest and could have passed between the lander and the sun. Depending on the dispersion of the cloud, a shadow would therefore be cast on the lander within a few seconds to a minute or so after touchdown. The first picture of the footpad commenced 25 seconds after landing, and shows a shaded vertical band at a time approximately 40 seconds later. It seems quite possible, therefore, that the streaks in the first martian picture frame (12 A 001/000) are due to the landing dust clouds passing between the sun and the scene in view at the time the camera was scanning this portion of the frame. In addition, the noise in the first few seconds of the first picture may have been caused by the imaging of coarse particles falling out of the dust cloud.

Soil fillets or tails, generally ascribable to aerodynamic processes, are visible adjacent to a number of Mars rock fragments. The direction of these tails is parallel either to wind direction or to the pattern of exhaust gases from the nearest descent engine (engine 2) and may depend on both sources. In this area [near footpad 3 (see Figs. 1 and 2)] the tails are generally parallel to the currently prevailing northeast winds and are also approximately radial to descent engine 2. Discrimination is therefore difficult, although it appears more likely that they have developed in the prevailing wind.

In the course of the site alteration tests in 1971, rocks located at a distance of 0.6 m from the descent engine axis were moved by the exhaust gas; the largest of these had a (terrestrial) weight of 74 g and was roughly equidimensional with a size of about 3.0 cm. The pressure required to move this rock was approximately 0.7×10^3 newton/m^2 (0.10 pound per square inch). The rock traveled 1.65 m from the engine axis; an initial pressure of about 0.35×10^3 newton/m^2 was required to keep it moving at this distance. On Mars, a rock of the same dimensions and density would weigh 0.38 times as much as the rock on Earth. With the same engine pressure conditions, therefore, larger rocks will be moved on Mars if they are not embedded. At a radial distance of 0.61 m from a descent engine axis on Mars, equidimensional loose rocks with dimensions up to about 7.0 cm would be moved under the nominal descent engine thrust conditions. At distances of 1.65 m on Mars, rock fragments on the surface up to dimensions of about 3.5 cm would be moved.

In the first image made after landing, several rocks which appear to be resting on the surface may have in fact been moved to their present positions by the engine exhaust gases. One such fragment appears at location 1 in Fig. 2. It is about 1.6 m from engine 2 and is estimated to weigh about 80 g on Mars. It could have been moved by the engine to its present position if it had been initially about 0.60 m or closer to the engine axis, for example at location 2, where a remnant fillet of soil appears to indicate the former presence of a rock. Other rocks that may have been moved are shown at location 3. Smaller loose rocks at the martian surface close to the engine axis could have been lifted off the surface, traveled through the martian atmosphere, and landed nearby. The soil seen in the footpad is additional evidence of soil moved during the landing either by footpad impact or engine-induced erosion. This finding is dramatic indication that some of the particles are less than 1 mm in diameter.

A view of the area below engine 2 was obtained by means of the mirror mounted on the side of the surface sampler. In this picture (Fig. 1), two small depressions are apparent. They occur at a spacing and in locations consistent with their formation by the jets out of two of the nozzles of engine 2. This appears to indicate that the grain size and cohesion of the surface material are different from those of the lunar nominal soil used in the site alteration tests. Since the grain size is below the resolution of the high-resolution frames, it is finer and has a broader range of sizes than the dune sand of the tests. This result may demonstrate that the finer grains are not as small as those of the lunar nominal material.

Interaction of the footpads with the martian surface. Although there is no distinct visual evidence of disturbance of the surface (by the footpad) in the area adjacent to footpad 3 (some of the apparently unsettled rock fragments may have been moved by the pad), analysis of the

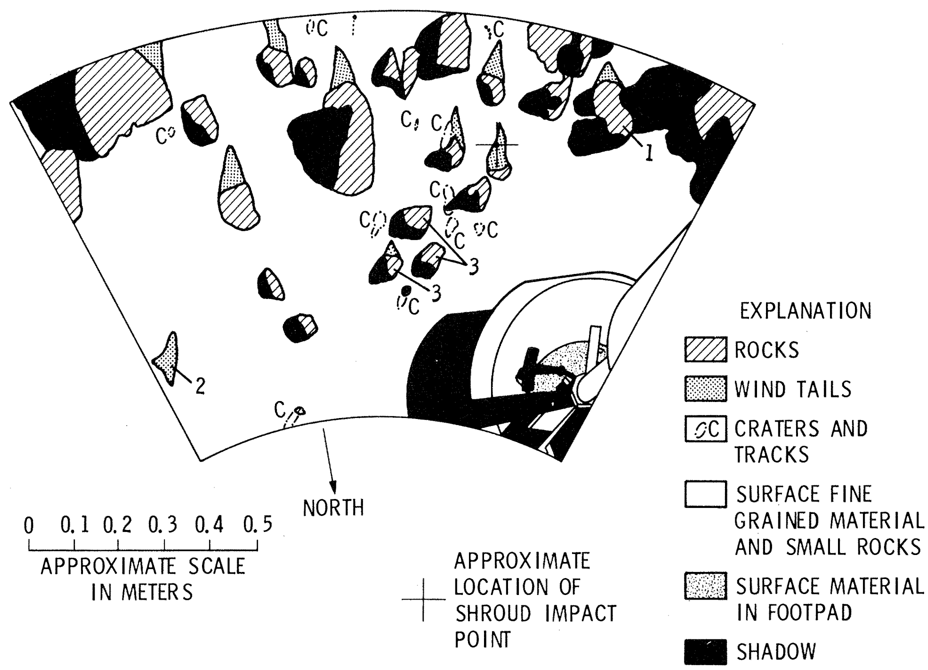

Fig. 2. Map of the area in Fig. 3 (on an orthographic projection) showing footpad, rocks, fillets (wind tails), debris in footpad, small craters and tracks, and the location of shroud impact crater. Rocks appear longer than they actually are because of the type of projection. This map was prepared from an image obtained prior to shroud impact. Numbers correspond to selected objects referred to in the text.

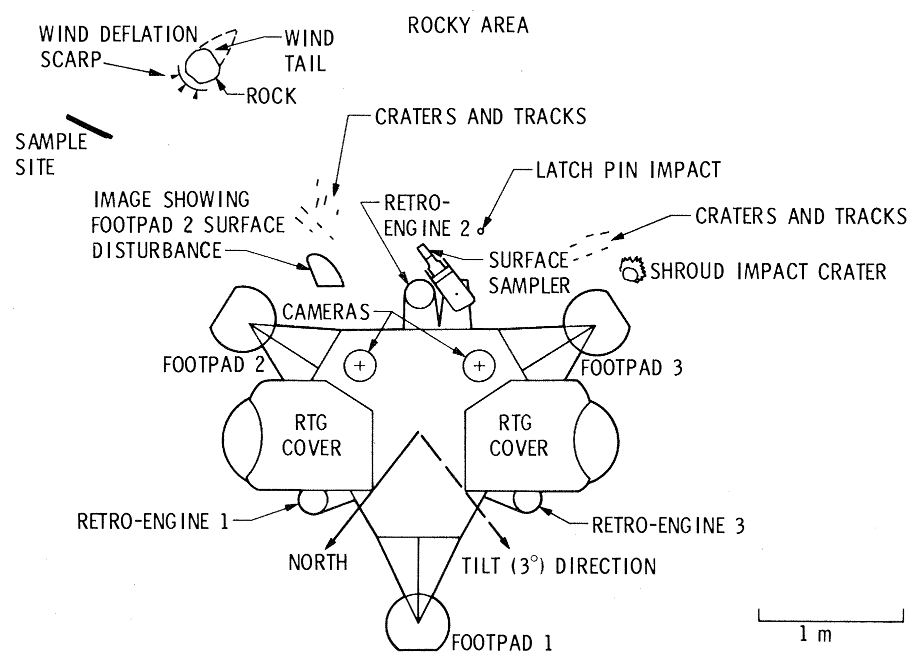

Fig. 3. Plan view of Viking 1 lander showing the spacecraft orientation, salient spacecraft parts, and location of surface disturbances and natural features relevant to the physical properties experiment. Location of the site where the surface sample was collected on sol 8 (28 July) is also shown; *RTG*, radioisotope thermoelectric generator.

shadow of the footpad on the adjacent surface indicates that the footpad has penetrated the martian material to a depth of about 3.6 cm. Unfortunately, footpad 1 cannot be viewed by the imaging system (see Fig. 3).

To date, no image of footpad 2 has been obtained, and so it is not possible to describe its attitude with respect to the surface. However, one high-resolution image in the vicinity of footpad 2 was returned; the area in the bottom left corner of this picture (see Fig. 4) is about 1.4 m from the center of footpad 2, which is 0.45 m in diameter. The surface in this picture is quite different from that in the neighborhood of footpad 3, lacking the rock fragment distribution. This surface (near footpad 2), by contrast, appears to be a relatively fine-grained soil surface, exhibiting only a few rocks (in the upper part of the picture). In the image are several additional features of interest. At the bottom left corner is a region of disturbed soil, intersected by a number of cracks or fractures running nearly parallel to the left edge of the frame. In all parts of the picture are small pits and tracks made by the impact of rock fragments or soil clods ejected by descent engine exhaust gas. From preflight tests and other data, it seems likely that such particles with dimensions of up to a few millimeters may have velocities in flight of up to several tens of meters per second. The tracks appear to belong to two groups which can tentatively be identified with ejecta from the directions of descent engines 1 and 2, respectively. The presence of the pits and tracks, assuming a particle velocity range, gives some information on the mechanical properties of the top few millimeters of surface material which in this region appears to be weaker and more porous than the soil around footpad 3.

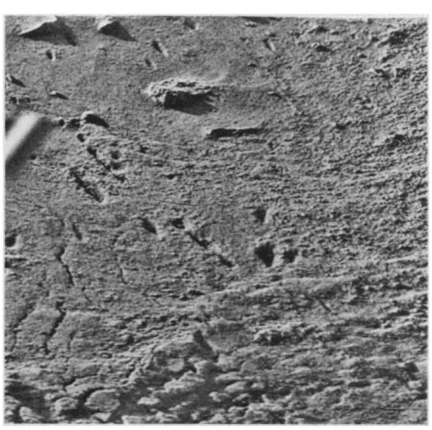

Fig. 4. Lander camera image showing the area believed to be disturbed by the interaction of footpad 2 with the martian surface and small rimmed pits, some of which contain small fragments, produced by small fragments propelled by the engine exhaust gases (event L.L.T. 004 071159; Fr 11 A 022/004; sun elevation angle is 22.5°, sun is to the upper left). Lower width of picture, ~23 cm; upper width, ~50 cm.

Table 1. Leg stroke and footpad penetration.

Leg number	Leg stroke (cm)	Footpad penetration (cm)
1	7.0 ± 0.6	No data
2	3.2 ± 0.6	Image not yet taken
3	8.3 ± 0.6	3.6

Although the disturbed area and cracks may be natural features, they occur so close to the spacecraft that they can be more plausibly attributed to interaction of the vehicle with the surface. In particular, it seems possible to relate the disturbed area at the bottom of the frame (Fig. 4) to the penetration of footpad 2 into the martian surface soil. A disturbance as extensive as that observed (1.3 m from the center of the footpad) implies a considerable depth of penetration of footpad 2 into soil less strong than that observed around footpad 3. Alternatively, the surface material may be the same, in which case it was less displaced by the footpad impact. The question of the provenance of the disturbance and cracks in the frame in question will ultimately be resolved by imaging of footpad 2. Penetration of an object such as a footpad into a relatively dense, slightly cohesive granular material is generally accompanied by bulging and cracking of the soil to a distance from the footpad which depends on the soil properties. With additional pictures these properties can be identified more closely.

Significance of stroke gauge extensions. The Viking 1 spacecraft landed on the martian surface at a vertical velocity of 2.5 m/sec with a lateral component of less than 0.15 m/sec. After the lander came to rest, leg 1 was oriented 38.1° west of north and tilted 2.99° from the local gravity vector. The downslope direction of tilt was 36.7° west of leg 1 (*9*) (see Fig. 3).

The kinetic energy prevailing at touchdown was absorbed by the crushing of elements in the leg struts during leg stroking and by deforming of the surface material around the footpads. The stroke of each of the primary struts was obtained from images of the three stroke gauges. The penetration of footpad 3 was deduced from the shadow cast by the outer edge of the footpad on the martian surface. Preliminary estimates of stroke and penetration are listed in Table 1. The strokes in Table 1 indicate that the plane through the three footpad attachment points is tilted about 2° relative to the top of the lander. Since the lander is tilted about 3° relative to the local horizontal, the footpad plane (an approximation to the local surface plane) is tilted about 1° relative to the local horizontal.

A comparison of the footpad penetration and leg strokes in Table 1 with theoretical predictions imply that the surface material is a little stiffer than the lunar nominal soil model (the average density was 1.67 to 1.8 g/cm^3) (*10*) and much stiffer than the most porous and weakly cohesive soil models considered during the design of the landing gear system. The theoretical landing dynamic behavior of the lander used in these preliminary comparisons was based on a vertical landing onto a horizontal surface. The prediction model made use of footpad penetration data obtained from static tests of a 3/8 model footpad penetrating various model soils, along with geometrical and load stroke properties of the landing gear.

Shroud impact. In the morning of sol 2, a shroud covering the surface sampler collector head was ejected by eight springs along a trajectory inclined downward about 40° from the local horizontal. High-speed camera photographs of shroud ejection on Earth indicate an initial velocity of 3.2 m/sec. Although the final velocity at impact on Earth is 4.6 m/sec, the reduced gravity on Mars implies a smaller velocity at impact (3.6 m/sec) and a larger range from the launch site. This larger range is in fact the case because the location of the impact crater produced by the shroud (see Figs. 1 and 2) is well beyond the footpad, as it

Fig. 5. Enlarged image showing the latch pin (8 cm long) on the martian surface (indicated by arrow). Note the small crater and disturbed surface around the pin (event L.L.T. 005 115359, Fr 12 A 033/005; sun elevation angle is 69.6°, sun is to the left).

should be in a reduced gravity field. Possible effects due to local topography have not yet been fully analyzed.

The 480-g shroud, which is a hollow cannister with metal plate tip, produced a crater about 1 cm deep and 9 cm in diameter by the displacement of rocks and the ejection of fine debris. Unlike the case in Earth-based tests, the shroud ricocheted from the field of view in the image shown in Fig. 1.

Latch pin impact. The boom latch pin of the surface sampler, which failed to release at the scheduled time, ultimately fell to the martian surface (see Fig. 3) from an estimated height of between 1.0 and 0.9 m in the morning of sol 5 (*11*). The velocity at impact from this height at the surface of Mars is between 2.7 and 2.6 m/sec and is equivalent to a fall height near 0.36 m on Earth. The pin, a slender (8.2 cm long, 0.6 cm in diameter, and 11.3 g) rod, impacted on an end with two roller bearings and then fell over toward the spacecraft. Upon impact a small circular crater about the size of the roller bearings was produced (see Fig. 5) by the ejection of dark, very fine-grained material (probably silt size) to distances of 2.4 cm from the crater center where the rollers hit. The remainder of the pin fell toward the spacecraft, producing an elongate depression by the ejection of dark material to distances of 1.5 cm from its axis. The pin now rests in this depression (Fig. 5).

Although the exact orientation of the pin at impact is unknown, the crater, depressions, and their ejecta are consistent with those of terrestrial materials with very low cohesions, a small grain size, and reasonable densities (1.2 to 1.7 g/cm^3).

Surface temperature measurements. A temperature sensor (thermocouple) attached to the inboard side of footpad 2 was used to measure ambient temperature during the parachute phase of the landing (*12*). Its survival depended on a soft landing, which indeed was the case. Temperature readings are being recorded periodically during the day and night. Since the sensor cannot be seen directly, it is not known whether the sensor is covered with surface material. Images of the sensor will be obtained by use of a mirror on the surface sampler later in the mission to aid in the interpretation of the data.

This first report on the physical properties of the martian surface must be considered preliminary. More refined measurements are to be made, based on stroke gauge extension, footpad penetrations, stereo images of the landing site area, and other new data such as motor currents during trenching and comminution. As these data are obtained, better values of the surface properties can be reported.

RICHARD W. SHORTHILL
University of Utah Research Institute, Salt Lake City 84108
ROBERT E. HUTTON
Applied Mathematics Laboratory, TRW Systems Group, Redondo Beach, California 90278
HENRY J. MOORE, II
U.S. Geological Survey, Menlo Park, California 90278
RONALD F. SCOTT
Department of Engineering and Applied Sciences, California Institute of Technology, Pasadena 91125
CARY R. SPITZER
NASA Langley Research Center, Hampton, Virginia 23665

References and Notes

1. M. H. Carr, H. Masursky, W. A. Baum, K. R. Blasius, G. Briggs, J. A. Cutts, T. C. Duxbury, R. Greeley, J. E. Guest, B. A. Smith, L. A. Soderblom, J. B. Wellman, J. Veverka, *Science* **193**, 766 (1976).
2. T. A. Mutch, A. B. Binder, F. O. Huck, E. C. Levinthal, S. Liebes, E. C. Morris, W. R. Patterson, J. B. Pollack, C. Sagan, G. R. Taylor, *ibid.*, p. 791.
3. Surveyor Program Results, *NASA SP-184* (1969).
4. Laboratory tests were carried out at the Langley Research Center under martian atmospheric conditions with different soil models.
5. The lunar nominal soil model is an artificially prepared soil having a particle size distribution based on screen analysis provided by the results of the Apollo 11 mission. The technique employed in the fabrication of the lunar nominal model was to take volcanic rock aggregate in the size range of from 5 cm to pan size from Table Mountain, Golden, Colorado, and grind it in an allochthonous mill charged with a few steel-alloy balls. The fine fraction of the model was separated in discrete size fractions by an air classifier. The coarse-sized particles were separated by screening. The crushed rock product was then blended in individual 55-gallon (208-liter) covered steel drums to achieve the desired particle size distribution for each drum.
6. The dune sand soil model is a natural occurring dune sand of volcanic origin. The material was collected near Sunset Crater, Arizona, in the Elden Ranger District of the Coconino National Forest.
7. We prepared the lunar nominal soil originally by placing it in 7.5-cm layers in the containers. Each layer was rolled several times with a garden roller to compact it. The final bulk density obtained for the material was in the range 1.7 to 1.8 g/cm^3.
8. S. L. Hess, R. M. Henry, C. B. Leovy, J. A. Ryan, J. E. Tillman, T. E. Chamberlain, H. L. Cole, R. G. Dutton, G. C. Grune, W. E. Simon, J. L. Mitchell, *Science* **193**, 788 (1976).
9. Data were obtained by the lander performance analysis group from the inertial platform data which remained operational for 15 seconds after touchdown.
10. Viking Lander "As Built" Performance Capabilities, *NAS1-9000* (June 1976), p. XII-II.
11. The normal sequence was modified because of the failure of the boom latching pin to drop out as the boom extended. The boom was subsequently commanded to extend farther, resulting in normal operation and the ejection of the pin.
12. A. O. Nier, W. B. Hanson, A. Seiff, M. B. McElroy, N. W. Spencer, R. J. Duckett, T. C. D. Knight, W. S. Cook, *Science* **193**, 786 (1976).
13. We acknowledge the continued aid and support given to the physical properties team by L. V. Clark, D. S. Crouch, L. K. Schwab, K. Z. Bradford, and W. DeShazor of the surface sampler team. The imaging team kindly furnished the images used in this report. We thank Dr. R. B. Hargraves who gave us able assistance throughout the mission and reviewed this manuscript. Work was supported by the National Aeronautics and Space Administration.

30 July 1976

The Viking Landing Sites: Selection and Certification

Abstract. *During the past several years the Viking project developed plans to use Viking orbiter instruments and Earth-based radar to certify the suitability of the landing sites selected as the safest and most scientifically rewarding using Mariner 9 data. During June and July 1976, the Earth-based radar and orbital spacecraft observations of some of the prime and backup sites were completed. The results of these combined observations indicated that the Viking 1 prime landing area in the Chryse region of Mars is geologically varied and possibly more hazardous than expected, and was not certifiable as a site for the Viking 1 landing. Consequently, the site certification effort had to be drastically modified and lengthened to search for a site that might be safe enough to attempt to land. The selected site considered at 47.5°W,22.4°N represented a compromise between desirable characteristics observed with visual images and those inferred from Earth-based radar. It lies in the Chryse region about 900 kilometers northwest of the original site. Viking 1 landed successfully at this site on 20 July 1976.*

The initial plans for site selection included the identification of a prime and a backup landing site for each spacecraft (*1*), and an additional pair of sites to be used as a contingency, selected primarily on the basis of safety. Areas near the prime and backup sites for the Viking 1 lander were first observed by Earth-based radar in 1967 and in the period from May to July 1976—about the time of insertion of the spacecraft into orbit about Mars. The northerly sites considered for the second lander are not observable by radar at any time, and are considered therefore as somewhat more of a risk. The third pair of sites was selected where they could be readily observed by Earth-based radar, and could be used in the event that the first landing was unsuccessful. These preselected site locations